30th Annual International IEEE EMBS Conference
Vancouver, British Columbia, Canada, August 20-24, 2008

Towards Detecting Surgical Clips in 3D Ultrasound for Target Localization in Radiation Therapy: a Study on Tissue Phantoms

Zahra Karimaghaloo, Prasad Shrawane, *Student Member, IEEE,* Purang Abolmaesumi, *Member, IEEE*, Gabor Fichtinger, *Member, IEEE*, Robert Rohling, *Member, IEEE*,

***Abstract* – A study is performed to measure the visibility of small surgical clips in 3D ultrasound volumes of a phantom as the first step towards using such clips as fiducial markers in radiation therapy. Visibility is calculated as the contrast to noise ratio of the echo from the clip to the background. The appearance of a resonance tail is also calculated using a moment analysis. Contrast is found to be high and mostly independent of material and size of the clip. All clips are visible, but the length of the tail is found to be dependent on clip orientation to the ultrasound beam. The consistent visibility of the clips suggests they are suitable as fiducial markers in ultrasound and the dependency of the resonance tail on orientation provides an opportunity to distinguish clips from other specular reflectors.**

I. INTRODUCTION

Accurate localization of the target volume is a key factor in the success of radiation therapy. One example is the localization of the lumpectomy site in the breast for electron boost irradiation [1]. The implantation of surgical clips and subsequent radiography is considered the gold standard for volume localization. In comparison to x-ray radiography, ultrasound has the advantages of being non-ionizing, easy-to-acquire and inexpensive. Ultrasound can be used in lieu of surgical clips and radiography by viewing the target directly [1], but some researchers have reported inadequate accuracy [2,3]. Surgical clips can also be detected in ultrasound images so it may be possible to combine the high accuracy of surgical clips with the advantages of ultrasound. Ultrasound may also be used to guide placement of the surgical clips [4].

Standard ultrasound creates 2D cross-sectional images so detection of clips would require accurate alignment of each clip with the cross-sectional plane. 3D ultrasound creates volumetric datasets so the need for alignment is reduced and multiple clips may be detected within a single volume. For these reasons, 3D ultrasound may be a more convenient way to detect and localize surgical clips for radiation therapy. The localization accuracy of thin wire, similar to these clips, has already been shown to be of the magnitude of the sub-millimeter range of the ultrasound axial resolution [5]. This paper investigates the issue of visibility of the clips.

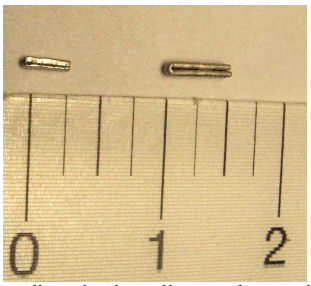

Fig.1 Small and medium titanium clips are shown with a scale of cm.

Surgical clips are manufactured in a variety of sizes and materials so different clips may have different visibility in ultrasound. Their appearance may also be dependent on the location and orientation of the clip with respect to the ultrasound probe. This paper investigates the appearance of several types and sizes of surgical clips. Tests are performed in the controlled environment of tissue-mimicking phantom to determine which factors affect visibility in 3D ultrasound.

II. METHOD

Three materials of surgical clips are tested: titanium, tantalum and stainless steel. Two clips are illustrated in Fig. 1. The approximate dimensions of the clips are 3 mm × 1 mm. These are referred to as "small clips". A fourth set of titanium "medium clips" (6 mm × 1 mm) are also tested. For each type of clip, a tissue-mimicking phantom is constructed with three embedded clips. Each clip is embedded at the same orientation but at different locations. The three locations are used to place a clip in each of the near-field, focus and far-field regions of the ultrasound image. The geometry of the phantoms is shown in Figs. 2 and 3. The locations of the clips ensure one clip does not obscure another clip, and allow ultrasound images to be taken from different faces of the phantom. This arrangement provides the necessary range of ultrasound images to be acquired without the need to construct multiple phantoms. The use of a single phantom for each type of clip also reduces the influence of variations in phantom construction when comparing results.

The phantom material is PVC (poly-vinyl chloride), a commonly used tissue-mimicking material in ultrasound research [6]. The speed of sound, attenuation and stiffness are in the same range as human tissue. The phantom is constructed by pouring heated PVC layer-by-layer into a

This work is supported by NSERC and CIHR. The authors also like to thank Narges Ahmidi for help with data analysis.

Z. Karimaghaloo is with the Department of Electrical and Computer Engineering, Queens University, Kingston, ON, Canada, K7L 3N6.
P. Abolmaesumi and G. Fichtinger are with the School of Computing, Queen's University, Kingston, ON, Canada, K7L 3N6.
P. Shrawane and R. Rohling are with the Department of Electrical and Computer Engineering, University of British Columbia, Vancouver, BC, Canada, V6T 1Z4. (Corresponding author: R. Rohling rohling@ece.ubc.ca)

custom-designed mold. Three layers plus a covering layer are used for the three clips. After each layer is poured and allowed to cool slightly, a clip is placed on the gel surface. By pouring the next layer before complete cooling of the previous layer is complete, the layers adhere completely. This ensures the transitions between layers are not visible in the ultrasound, only the clips are visible. Four phantoms are constructed for the four types of clips.

Ultrasound images are acquired with the Voluson 730 Expert (General Electric Health Care, Chalfont St. Giles, UK). A 3D linear array transducer (RSP5-12) is used to acquire 3D ultrasound volumes of the phantoms. The transducer has a footprint of 38.4 mm × 44.5 mm and the depth setting ranged from 34 mm to 79 mm depending on clip location. The probe acquires a 3D volume by sweeping a 2D transducer through an angle of 29° to acquire 181 slices. As mentioned in the Introduction, a benefit of using a 3D ultrasound probe, compared to a standard 2D cross-sectional probe, is the elimination of operator dependency on image quality by removing the need to manually align the clip within a plane. The 3D probe automatically scans a substantial volume so the clip is easily situated within the volume. Automated analysis can then be performed on the full 3D volumetric data.

The set of 2D swept slices are reconstructed into a regular 3D Cartesian volume by 3D View 2000 software (General Electric Health Care). The probe is held on different faces of the phantom to acquire volumes of the clips in the axial, lateral and elevational orientations (corresponding to x, y, and z axes of the Cartesian volumes). Three ultrasound volumes are repeated for each combination of clip type and orientation so that an estimate of measurement error is made.

Two measures of visibility are proposed. First, the contrast-to-noise ratio (CNR) is used to measure clip contrast. This measure has been commonly used for lesion detectability in ultrasound [7]. It encompasses both the brightness of the clip and the variations of the clip brightness and the background intensities. Practical suggestions for calculating CNR for the region of interest were taken from [8]. In general, the clips are depicted as bright structures within a darker background. Some slices of the volume occasionally contain a high level of noise that arises from the practical limits on phantom size and construction (reflections from walls), so were removed manually. We define the mean value of the bright pixels by selecting a threshold and averaging the n values found above the threshold:

$$\mu_{bright} = \frac{1}{n}\sum_{i=1}^{n}\mu_i \ .$$

Similarly, for the dark background, the mean value is calculated with the m values found below a threshold:

$$\mu_{dark} = \frac{1}{m}\sum_{j=1}^{m}\mu_i \ .$$

Using the same pixels in the above calculations, the variances σ^2_{bright} and σ^2_{dark} are calculated. If we define the contrast of the clips as the relative difference between the mean values of the bright and dark regions, then CNR can be defined as

$$CNR = \frac{contrast}{noise} = \frac{\mu_{bright} - \mu_{dark}}{\sqrt{\sigma^2_{bright} + \sigma^2_{dark}}} .$$

The thresholds are set according to the brightest point in the volume, so the thresholds are recalculated for each volume. In practice, the brightest points ranged from 100 to 200 (out of a maximum of 255), and the threshold is set around 70. Since the background was generally much lower than 70, this is a conservative threshold. The background threshold is set to 5, 10 or 15 depending on the volume. The exact values of the thresholds, since kept within reasonable ranges, have an insignificant effect on the CNR calculations.

The second measure of visibility is related to the resonance "tail" that often appears below the clip in the axial direction of the acoustic beam. Measurement of the ultrasound resonance phenomenon has been investigated previously for brachytherapy seeds [9]. The issue of visibility and localization of brachytherapy seeds is similar to the problem of clip visibility here, and the size and shape of the brachytherapy seeds are similar to the clips used in this study. In [9], a characteristic "signature" was measured for the seeds using a singular spectrum analysis of the radiofrequency ultrasound signals. Here, a simpler measure is proposed based on measurements of the B-mode intensity.

The length of the resonance tail is measured by first calculating the components of the centroid of the echo from the clip using the central moments of voxels above a threshold. A threshold of 70 is used for all volumes, but any value within the range of 50 to 100 generates near identical results. The thresholded voxels are then normalized to the maximum intensity. The length of the tail is then defined as the variance of the thresholded voxel values below the clip (in the axial direction):

$$tail = \frac{1}{p}\sum_{u=1}^{p}\mu_u (y_u - y_c)^2$$

where y_u is the axial location of a voxel u, y_c is the axial component of the centroid and μ_u is the normalized voxel intensity value. The index u covers all thresholded voxels below the centroid (total p).

In summary, the CNR and length of the resonance tail are calculated for the three clip orientations (axial, lateral, elevational) and three locations (near-field, focus, and far-fields) for a total of nine cases. The CNR and the tail are calculated three times from the three repeated scans and then averaged. The results are then tabulated for each of the nine cases versus four clip types.

III. RESULTS AND DISCUSSION

Example ultrasound images are shown in Fig. 4. The clips were discernable as bright features in all ultrasound volumes. The CNR values are given in Table I. Using the two-sample t-test for equal means, no significant difference was found between the means of the CNR for the four clip types (α=0.05). This means that all three materials and both sizes produced equal visibility on average over all cases.

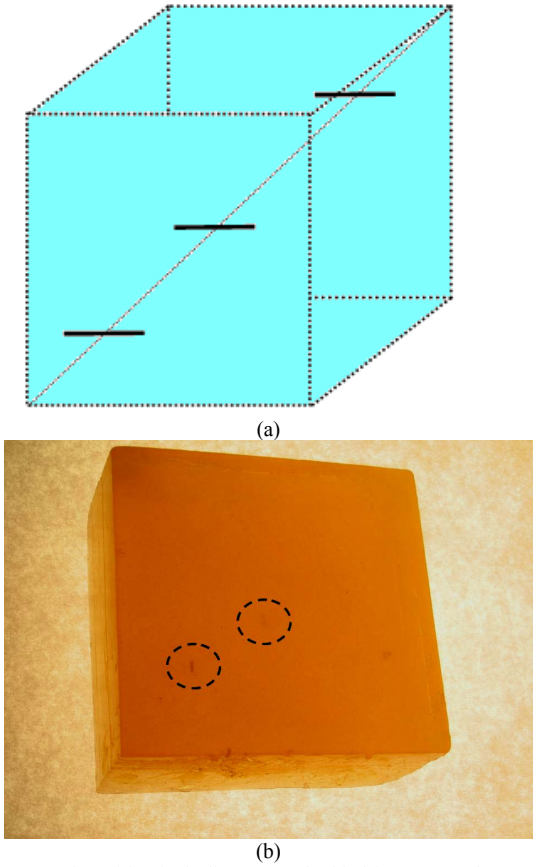

(a)

(b)

Fig.2 (a) Three identical clips are embedded in a PVC phantom at locations that correspond to the near-, focal- and far-field regions of the ultrasound image. The clips are also displaced laterally so that one clip does not obscure an underlying clip. The clip size is exaggerated for clarity. (b) The phantom material is semitransparent to aid placement of ultrasound probe above each clip. Two of the three clips are barely visible in the circled regions of the photograph.

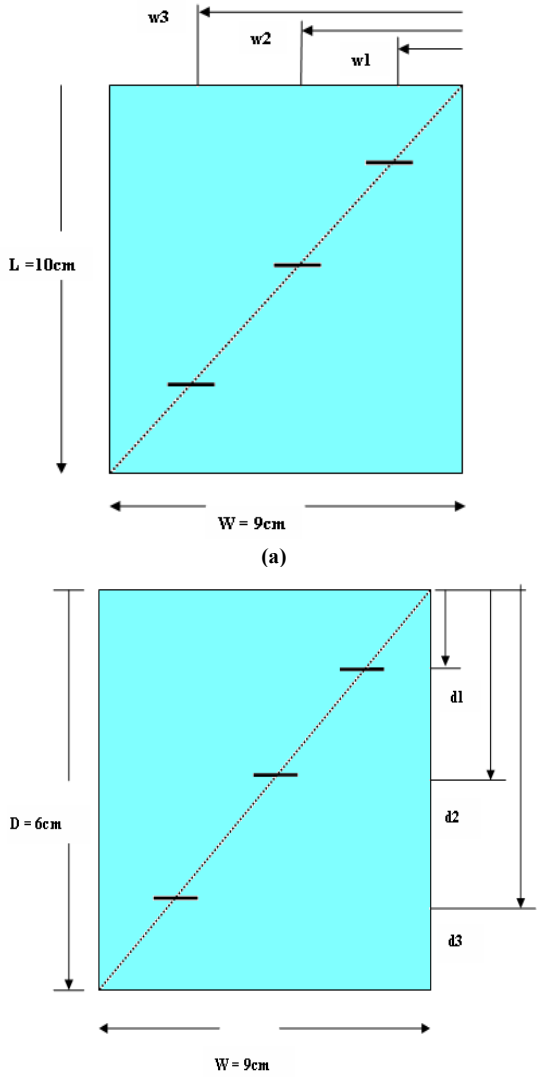

Fig.3 The locations of the clips are as shown in (a) top view and (b) side view. The outside dimensions of the phantom are 90 mm × 100 mm × 60 mm. In the top view (a), the clips are located at w_1=20mm, w_2=43mm, w_3=64mm. In the side view (b), the clips are located at d_1=18mm, d_2=32mm, d_3=43mm.

Looking at each clip type independently, the CNR was significantly greater in the focus than the far-field for the small titanium, small stainless-steel and medium titanium clips. This was calculated on average over all orientations. The small stainless-steel clips also showed a significantly greater CNR in the near-field than the focus.

Again, looking at each clip type independently, the CNR was significantly better for the axial orientation than the lateral or elevational direction only for the medium titanium clip. This was calculated on average over all locations. Clip orientation showed no significant difference in CNR for the other clip types.

In general, the clips showed a high CNR with only small variations with location and orientation. The decrease in CNR for the far-field is expected since ultrasound receives weaker echoes in the far-field, so noise is relatively larger. The resolution is also lower in the far-field so the clip is depicted with slightly more blurring. This also contributes to a lower CNR. Only one case showed a dependency of CNR with clip orientation (medium titanium clip). Otherwise the clips are visible clearly at all orientations.

The fact that all materials performed equally well may be a benefit. For example, titanium produces fewer artifacts than ferrous materials in CT and MR imaging [10], so may be preferred over stainless steel.

Measurements of resonance tail, given in Table II, show that the tail appears to be much more variable than CNR. There does not appear to be a dependency of the length of the tail with clip material, size, or location. The only dependency that can be discerned is that the axial orientation gives a longer tail than lateral or elevational directions, averaged over all materials, locations and sizes ($p<0.01$). There is still a fairly large variability in the length of the tail for axial orientations (standard deviation for all tests of axial orientations is 3.6 mm). We speculate that this variability comes from the sensitivity of the resonance to the angle of the seed with respect to the ultrasound beam; if not exactly aligned, less resonance is observed.

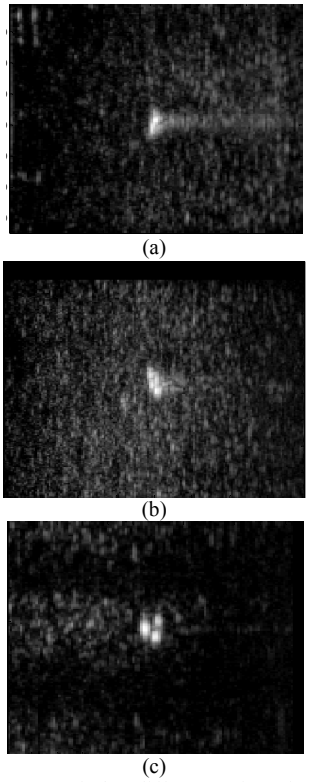

Fig.4 Sample images of the different orientations of the small tantalum clip in the near field. The images are extracted from the axial-lateral plane of the volume where rows are in the axial direction. The ultrasound source is from the left so the tail of the resonance points to the right. (a) axial orientation of clip. (b) lateral orientation of clip. (c) elevational orientation of clip.

The sensitivity of the appearance of brachytherapy seeds as a function of seed angle with respect to the ultrasound beam has been studied previously [11]. In that study, integrated optical density (IOD) was shown to change nonlinearly with seed angle in 2D ultrasound in a water bath. Although that study did not measure the resonance tail, given the dependency of IOD on angle, and our results, it may be feasible to use the variable appearance with respect to beam angle to distinguish a clip from other bright echoes, such as calcifications. For example, if the clip or seed can be viewed from more than one angle (such as with spatial compounding by electronic beam steering) then the change in the appearance as a function of beam angle may be compared to a model of the appearance of the clip. The comparison may be put into a probabilistic framework to help classify bright echoes as clips. Robust classification of markers remains a key unsolved clinical problem in ultrasound guided radiation therapy.

TABLE I

CNR VALUES FOR THE NINE CASES VERSUS FOUR CLIP TYPES. THE LABELS "TI", "TA" AND "SS" STAND FOR TITANIUM, TANTALUM AND STAINLESS STEEL RESPECTIVELY. BOTH "SMALL" AND "MEDIUM" SIZED CLIPS WERE STUDIED.

Case	Orientation	Location	Ti small	Ta small	SS small	Ti med
1	Axial	Near	9.0	7.2	10.2	10.5
2	Lateral	Near	8.7	7.1	8.7	9.0
3	Elevational	Near	10.4	8.3	7.2	8.4
4	Axial	Focal	8.2	6.7	6.8	7.1
5	Lateral	Focal	10.9	7.5	6.5	7.2
6	Elevational	Focal	7.6	4.6	6.0	8.4
7	Axial	Far	8.6	6.6	7.0	8.9
8	Lateral	Far	7.0	6.5	3.1	2.9
9	Elevational	Far	4.0	4.2	3.5	3.1

TABLE II

MEASURE OF LENGTH OF RESONANCE TAIL FOR THE NINE CASES VERSUS FOUR CLIP TYPES (EXPRESSED IN MILLIMETERS). THE LABELS "TI", "TA" AND "SS" STAND FOR TITANIUM, TANTALUM AND STAINLESS STEEL RESPECTIVELY. BOTH "SMALL" AND "MEDIUM" SIZED CLIPS WERE STUDIED.

Case	Orientation	Location	Ti small	Ta small	SS small	Ti med
1	Axial	Near	1. 87	11.33	1. 77	5. 50
2	Lateral	Near	0. 09	1. 2	0. 76	0. 48
3	Elevational	Near	0. 09	0. 41	0. 09	0. 10
4	Axial	Focal	6. 15	4. 41	4. 38	1. 27
5	Lateral	Focal	1. 00	0. 63	0. 67	0. 61
6	Elevational	Focal	0. 12	0.125	0. 09	0. 12
7	Axial	Far	3. 42	2. 96	3. 81	2. 41
8	Lateral	Far	0. 16	0. 36	0. 24	0. 95
9	Elevational	Far	0. 16	2. 48	1. 13	1. 87

REFERENCES

[1] J. Ringash, T. Whelan, E. Elliot, T. Minuk, K. Sanders, H. Lukka, H. Reiter, "Accuracy of ultrasound in localization of breast boost field," *Radiother Oncol*, vol. 72(1), 2004, pp.61-66.

[2] R. Rabinovitch, C. Finlayson, P. Zhaoxing, J. Lewin, S. Humphries, W. Biffl, R. Francoise, "Radiographic evaluation of surgical clips is better than ultrasound for defining the lumpectomy cavity in breast boost treatment planning: a prospective clinical study," *Int J Radiat Oncol Biol Phys*, vol. 47(2), 2000, pp. 313-317.

[3] J. A. Kim, M. Collver, K. Howell, K. Meyer, J.M. Johnson, J. Landercasper, P. J. Lambert, W. A. Frye, P. J. Havlik, "Comparison of localization methods of lumpectomy cavity for boost treatment in patients with breast-conserving therapy," *Gundersen Lutheran Medical Journal*, vol. 3(2), 2005, pp. 54-57.

[4] L. F. Baron, P. L. Baron, S. J. Ackerman, D. D. Durden, T. L. Pope, "Sonographically guided clip placement facilitates localization of breast cancer after neoadjuvant chemotherapy," *American Journal of Roentgenology*, vol. 174, 2000, pp. 539-540.

[5] A. K. Jain, R. H. Taylor, "Understanding bone responses in B-mode ultrasound images and automatic bone surface extraction using a Bayesian probabilistic framework", *Proc. SPIE* 5373, 2004, 131-142.

[6] B. Chan, J. V. Merton-Gaytrope, M. P. Kadaba, Z. Simindokht, D. Bryk, "Acoustic properties of polyvinyl chloride gelatin for use in ultrasonography," *Radiology* vol. 152(1), 1984, pp.215-216.

[7] P. F. Stetson, F. G. Sommer, A. Macovski, "Lesion contrast enhancement in medical ultrasound imaging," *IEEE Trans Med Imag*, vol. 16(4), 1997, pp.416-425.

[8] X. Song, B. W. Pogue, S. Jian, M. M. Doyley, H. Dehghani, T. D. Tosteson, K. D. Paulsen, "Automated region detection based on the contrast-to-noise ratio in near-infrared tomography," *Applied Optics*, vol. 43(5), 2004, pp. 1053-1062.

[9] J. Mamou, E. J. Feleppa, "Ultrasonic Imaging of brachytherapy seeds based on singular spectrum analysis," Proc. 2006 *IEEE Ultrasonics Symposium*, Vancouver, BC, 2006, pp. 1107-1110.

[10] J. C. Ho, C. Y. Wu, M. J. Carron, K. P. Maughan, F. J. Schmidt, "Titanium cerebral aneurysm clips: characterization and performance in magnetic resonance imaging and computed tomography," *Journal of Testing and Evaluation*, vol. 24(2), 1996, pp.85-90.

[11] B. J. Davis, R. R. Kinnick, M. Fatemi, E. P. Lief, R. A. Robb, J. F. Greenleaf, "Measurement of the ultrasound backscattering signal from three seed types as a function of incidence angle: application to permanent prostate brachytherapy," *Int J Radiat Oncol Biol Phys*, Vol. 57(4), 2003, pp. 1174-1182.